Order-*N* tight-binding molecular dynamics simulation with a Fermi operator expansion approach: application to a liquid carbon

2000 J. Phys.: Condens. Matter 12 1627

(http://iopscience.iop.org/0953-8984/12/8/305)

J. Phys.: Condens. Matter **12** (2000) 1627–1639. Printed in the UK PII: S0953-8984(00)07459-2

Order-N tight-binding molecular dynamics simulation with a Fermi operator expansion approach: application to a liquid carbon

T Oda and Y Hiwatari

Department of Computational Science, Faculty of Science, Kanazawa University, Kakuma-machi, Kanazawa 920-1192, Japan

Received 2 September 1999

Abstract. Order-N tight-binding molecular dynamics has been implemented with a Fermi operator expansion and applied to a low-density liquid carbon at a temperature above the melting point of graphite. For various sets of the parameters introduced in the order-N approximation, the radial distribution function and the mean square displacement are calculated. The conservation of energy during a constant-energy simulation is studied.

1. Introduction

Tight-binding (TB) molecular dynamics (MD) is a useful tool for investigating dynamical properties of clustering atoms and disordered materials. Since this method treats explicitly electronic states of a system as well as atomic configurations, it is applied to a broad class of materials to study dynamical properties of materials both at the microscopic and the electronic levels. The TB-MD should be compared with an *ab initio* MD, in which every quantity needed is calculated without free parameters. However, *ab initio* MD requires much larger computational resources and therefore involves a limitation on both the system size and the computational time. On the other hand a classical MD, in which much larger systems are possible, is restricted to only atomic structures.

The TB method usually requires matrix diagonalization and therefore the calculational cost is proportional to the cube of the system size ($\mathcal{O}(N^3)$). This explicit diagonalization restricts consideration to only small systems again. To break through this bottleneck, various $\mathcal{O}(N)$ schemes [1–5] have been proposed and microscopic accuracies have been investigated [1–6]. These $\mathcal{O}(N)$ schemes use a localization approximation in the target system. Qiu and co-workers [7] improved the density matrix method [1] developed by Li *et al* and applied the result to carbon systems. Stephan and Drabold [6] considered error estimations in detail for the Fermi operator expansion method (FOEM) and applied it to a first-principles Hamiltonian based on the local density approximation. Horsfield and co-workers [8, 9] implemented the bond-order potential method and examined the degree of accuracy in MD simulations as well as its parameter dependence. Horsfield and Bratkovsky [10] also investigated TB energies and atomic forces for finite electronic temperatures using the extrapolated electronic energy. Bowler *et al* [11] examined the accuracy and efficiency for several $\mathcal{O}(N)$ methods including the FOEM.

0953-8984/00/081627+13$30.00

The FOEM was originally developed to a usable level by Goedecker and co-workers [4,5]. Although it is not recommended as the best procedure for $\mathcal{O}(N)$ MD simulations of liquid materials in the paper of Bowler *et al* [11], it has a very simple algorithm structure and turns out to be suitable for making calculations with a massive parallel architecture.

In this paper an $\mathcal{O}(N)$ TB-MD, with the FOEM [5], is implemented and MD simulations for a low-density liquid carbon are presented for various parameters introduced in the $\mathcal{O}(N)$ approximation. We checked the accuracy of the conservation of energy to see the quality of the simulations. A brief review of the FOEM is presented in section 2 and the algorithm in section 3. Section 4 is devoted to results of simulations and discussion of the FOEM.

2. Fermi operator expansion

In the TB-MD, it is required to calculate the band energy, which is the sum of eigenvalues up to the Fermi level with the weight of the Fermi distribution:

$$E_{\mathrm{tb}} = 2\sum_i \varepsilon_i f\left(\frac{\varepsilon_i - \mu}{\Delta\varepsilon}\right) \tag{1}$$

where ε_i is the ith eigenvalue of the TB Hamiltonian $\mathcal{H}$, f is the Fermi distribution function—namely, $f(y) = 1/(\mathrm{e}^y + 1)$—and μ is the chemical potential. The latter is determined so as to satisfy the charge neutrality. The factor 2 in (1) comes from spin degeneracy. The smearing width of the Fermi level, $\Delta\varepsilon$, is interpreted in two ways. One is as a realistic electronic temperature and the other is as an artifact introduced to stabilize the calculation. One possible choice of $\Delta\varepsilon$ is to make it coincide with the physical temperature of the system. The derivative of the band energy with respect to atomic coordinates contributes to the force acting on the atoms, which is needed in MD simulation. The FOEM is briefly described only with the band energy here. The argument holds for the derivatives.

Alternatively, the band energy can be expressed in terms of the trace with any basis sets:

$$E_{\mathrm{tb}} = 2\,\mathrm{Tr}\,[\mathcal{H} f(x)] \tag{2}$$

where $x = (\mathcal{H} - \mu)/\Delta\varepsilon$. With an orthogonal TB basis, $\{\varphi_{\ell\alpha}\}$, this is rewritten as

$$E_{\mathrm{tb}} = 2\sum_{\ell\alpha}\sum_{\ell'\alpha'} \langle\varphi_{\ell\alpha}|\mathcal{H}|\varphi_{\ell'\alpha'}\rangle\langle\varphi_{\ell'\alpha'}|f(x)|\varphi_{\ell\alpha}\rangle \tag{3}$$

where $\varphi_{\ell\alpha}$ specifies the αth atomic orbital of the ℓth atom. Matrix elements of the Fermi operator $f(x)$ are calculated directly using a polynomial expression for $f(x)$. The Chebyshev polynomial, $\{T_j\}$, is used as usual [5]:

$$f(x) = f[t] = \frac{c_0}{2} + \sum_{j=1}^{n_{\mathrm{pl}}} c_j T_j(t) \tag{4}$$

where t is rescaled from x with the following relation:

$$x \equiv \frac{x_{\max} - x_{\min}}{2}\, t + \frac{1}{2}(x_{\max} + x_{\min}). \tag{5}$$

$x_{\max}$ and $x_{\min}$ are the maximum and the minimum eigenvalues of x. Note that the eigenvalue of t falls in the range between -1 and 1. The degree of the polynomial, n_{pl}, is chosen to be

$$n_{\mathrm{pl}} = CW/\Delta\varepsilon \tag{6}$$

where $W \sim 2\,\Delta\varepsilon \max(x_{\max}, |x_{\min}|)$ and C is a constant. Note that W is interpreted as a bandwidth of the electronic structure.

The expansion coefficients are set with the following formula:

$$c_j = \frac{2}{\pi}\int_{-1}^{1} f[p]T_j(p)\,\frac{\mathrm{d}p}{\sqrt{1-p^2}}. \tag{7}$$

In the practical implementation, we adopted $x_{\min} = -x_{\max}$ and used the following expression for the coefficients:

$$c_j = \begin{cases} 1 & \text{for } j = 0 \\ \dfrac{4}{\pi}\displaystyle\int_0^{p_1}\left(f[p]-\frac{1}{2}\right)T_j(p)\,\frac{\mathrm{d}p}{\sqrt{1-p^2}} - \frac{4}{\pi}\frac{\sin(j\theta_1)}{2j} & \text{for } j = \text{odd} \\ 0 & \text{otherwise} \end{cases} \tag{8}$$

where $p_1 = \cos(\theta_1)$ $(0 \leqslant \theta_1 \leqslant \pi/2)$. To deduce this expression we have taken into account the odd symmetry of $f[p] - \frac{1}{2}$ and approximated $f[p] - \frac{1}{2}$ as $\frac{1}{2}$ for $|p| \geqslant p_1$. Figure 1 shows

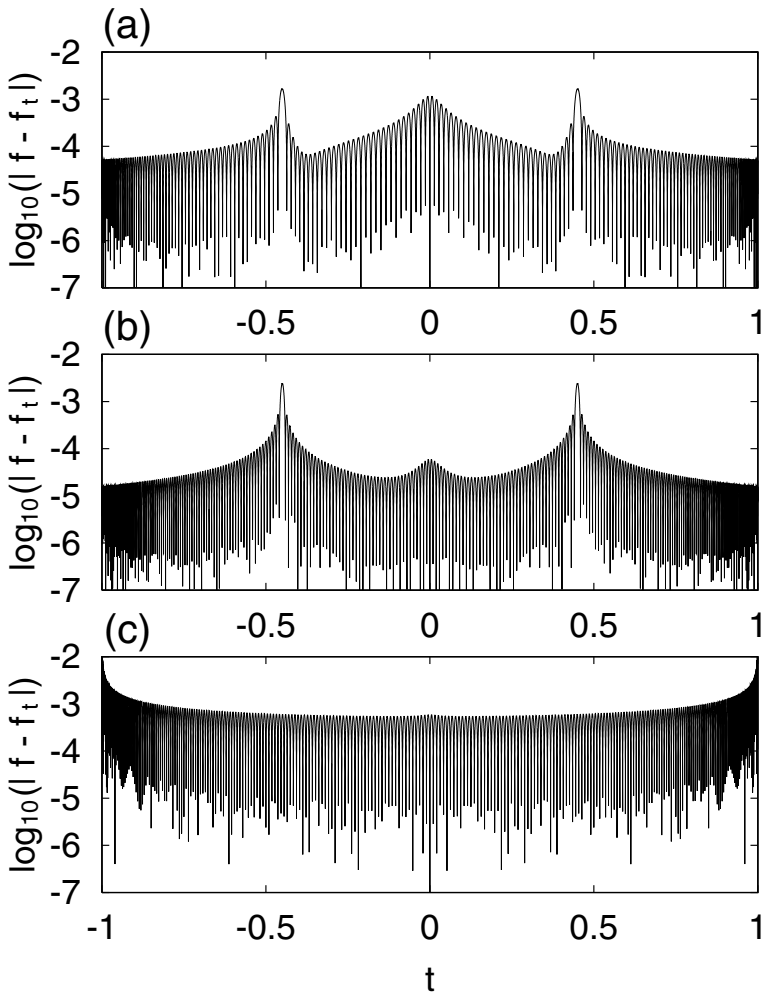

Figure 1. Errors caused by truncation of the Chebyshev polynomial for (a) $C = 1.0$ and $p_1 = 0.45$, (b) $C = 1.5$ and $p_1 = 0.45$, and (c) $C = 1.5$ and $p_1 = 1.0$. The other parameters are $x_{\max} = 100$, $\Delta\varepsilon = 0.5$ eV for all cases.

typical errors introduced by the truncation of a Chebyshev polynomial for $\Delta\varepsilon = 0.5$ eV and $x_{\max} = 100$. In figures 1(a) and 1(b), $C = 1.0$ and 1.5 are used, respectively, and $p_1 = 0.45$ for both cases. It turns out that the averaged errors are about 7×10^{-5} and 2×10^{-5}, respectively. In figure 1(c), $C = 1.5$ and $p_1 = 1$ are used. When $p_1 \sim 1$ the errors become obviously larger than in the case shown in figure 1(b) and the averaged error is about 4×10^{-4}. In the MD simulations of the present work, $p_1 = 0.45$ is used.

An important feature of the matrix elements of $f(x)$ is that they decrease exponentially as the distance between two orbitals increases [4,5]. This feature allows us to obtain an $\mathcal{O}(N)$ algorithm by introducing a localization region (LR) associated with each atom. Outside the LR, the amplitudes of the projected orbital defined by $f(x)|\varphi_{\ell\alpha}\rangle$ can be negligible. In the double summation in (3), one loop runs through all orbitals and atoms and the other loop can be truncated at the boundary of the LR. Denoting the averaged number of atoms in LRs as $N_{\mathrm{a}}^{\mathrm{LR}}$ and the number of atomic orbitals on one atom as N_{orbit}, the required amount of calculation on evaluating the band energy is proportional to $N N_{\mathrm{a}}^{\mathrm{LR}} N_{\mathrm{orbit}}^2 n_{\mathrm{pl}}$. Indeed, the most time-consuming part (at least 90%) of the present TB-MD simulation is calculating $f(x)|\varphi_{\ell\alpha}\rangle$, which mainly consists of n_{pl} matrix–vector multiplications [5]. One scalar product in each matrix–vector multiplication is proportional to the number of hoppings from a reference orbital to the orbitals of neighbours.

The LR is usually determined from the number of atoms in the region, the number of hoppings for the TB basis or the cut-off radius R_{cut} of the region. Because the latter procedure is the simplest, we adopted it for liquid carbons. The other two procedures may have some advantages in stabilizing the MD simulation in which the volume varies and in reducing the number of TB bases in a LR without loss of accuracy of the calculations.

Figure 2 demonstrates an $\mathcal{O}(N)$ scaling of the algorithm in using the Fermi operator expansion. Only the cpu time of the calculation for the band energy is plotted. It turns out that the $\mathcal{O}(N)$ scaling is obviously observed over a few hundred atoms.

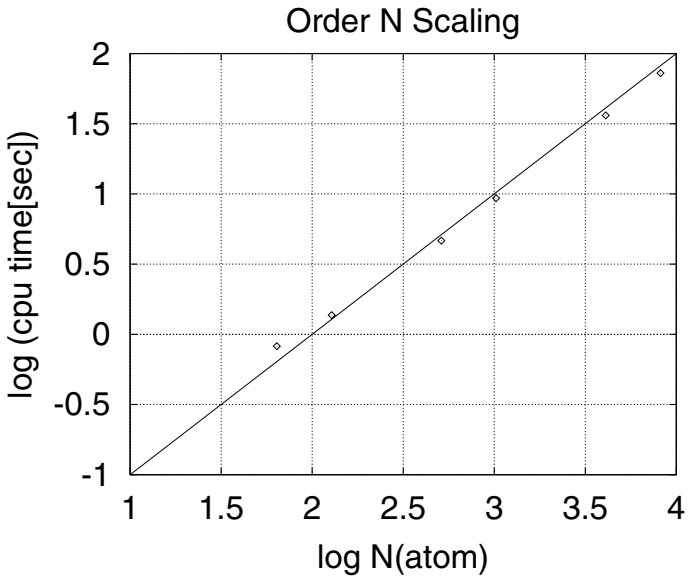

Figure 2. $\mathcal{O}(N)$ scaling of the FOEM implemented. Only the cpu time of the calculation for the band energy is shown. The straight line is a guide for the eyes.

3. Molecular dynamics

In the TB-MD implemented, time evolutions of atoms are described by a Lagrangian:

$$L = \sum_i \frac{1}{2} m_i \dot{\boldsymbol{r}}_i^2 - E_{\rm pot}[\{\boldsymbol{r}_i\}] - \mu(N_{\rm ele} - 2\,{\rm Tr}[f(x)]) \tag{9}$$

where

$$E_{\rm pot} = E_{\rm tb} + E_{\rm ent} + E_{\rm rep} \tag{10}$$

$$E_{\rm ent} = -2\,\Delta\varepsilon\,{\rm Tr}[s(x)] \tag{11}$$

$$s(x) = -\{f(x)\ln f(x) + (1 - f(x))\ln(1 - f(x))\}. \tag{12}$$

$N_{\rm ele}$ is the number of total valence electrons, and $E_{\rm rep}$ is the effective repulsive potential. The last term of (9) is nothing but the constraint of charge neutrality. The entropic energy of electrons associated with $s(x)$ in (11) is also introduced. Including this term in the potential energy $E_{\rm pot}$, the conservation energy can be defined:

$$E_{\rm cons} = \sum_i \frac{1}{2} m_i \dot{\boldsymbol{r}}_i^2 + E_{\rm pot} + \mu(N_{\rm ele} - 2\,{\rm Tr}[f(x)]). \tag{13}$$

The last term on the right-hand side is added to a conventional definition [12] but it should be vanishing when the charge neutrality is strictly satisfied. This definition gives us a smooth evolution of the conservation energy.

The equations of motion are obtained from L in (9) as

$$m_i \frac{{\rm d}^2 \boldsymbol{r}_i}{{\rm d}t^2} = \boldsymbol{F}_i \tag{14}$$

$$\boldsymbol{F}_i = -2\,{\rm Tr}\left[\frac{{\rm d}\mathcal{H}}{{\rm d}\boldsymbol{r}_i} f(x)\right] - \frac{{\rm d}E_{\rm rep}}{{\rm d}\boldsymbol{r}_i}. \tag{15}$$

In the MD implementation these equations are integrated with the Verlet algorithm. Matrix elements of $s(x)$ are evaluated by the same way as for $f(x)$ but with another set of expansion coefficients associated with the Chebyshev polynomial. The error arising from fitting is usually smaller by about one order of magnitude than that for $f(x)$.

The computational scheme adopted here, in which the charge neutrality is fulfilled at each MD step, is different from the scheme in [5], where the constant chemical potential and a smearing width around the Fermi level are used. A similar scheme in which a finite electronic temperature and an entropic energy are adopted was used with the diagonalization method (DM) to study liquid carbons [12]. To impose the constraint of the charge neutrality, the chemical potential is adjusted and, in doing this, a few iterations are usually needed in each MD step. These iterations require more cpu time. By lowering the tolerance on the charge neutrality, the number of iterations could be reduced. Some physical quantities, however, lose their accuracy.

The parameters ($R_{\rm cut}$, W, $\Delta\varepsilon$, and C) are introduced in the $\mathcal{O}(N)$ approximation. Two cases, $R_{\rm cut} = 0.55$ and 0.65 nm, are tested in the present work. Although these values are no larger than those used in the previous works [5, 6], the results of the present work also show a good level of accuracy. W is determined from the bandwidth of the electronic structures in the target system. A larger value of W gives stability of MD simulations, and perhaps accuracy of the calculations as well. On the other hand, it should be as small as possible to reduce $n_{\rm pl}$.

The smearing width $\Delta\varepsilon$ is ideally taken in accordance with a physical temperature. For much lower temperatures, however, the criterion for determining $n_{\rm pl}$ (see (6)) requires an impractical resource of calculations. For this case the modified potential energy extrapolated

to absolute zero may be efficient [10]. As a larger value of $\Delta\varepsilon$ is taken, a smaller value of $n_{\rm pl}$ is sufficient. In addition, if rapidly damped behaviours of $f(x)|\varphi_{\ell\alpha}\rangle$ are observed for larger values of $\Delta\varepsilon$, $R_{\rm cut}$ could be reduced simultaneously [11]. The value of C is directly related to the accuracy of the expansion and $C = 1.5$ results in a sufficient accuracy in the previous works [10, 11].

The temporal pressure in the TB-MD scheme, as is the case for the classical MD with atomic pair potentials, is represented by the form

$$P = \frac{1}{V}\left\{Nk_{\rm B}T - \frac{1}{6}\sum_{i,j}^{i\neq j}\boldsymbol{F}_{i,j}\cdot(\boldsymbol{r}_j - \boldsymbol{r}_i)\right\} \tag{16}$$

where $\boldsymbol{F}_{i,j}$ is the contribution indicated by the jth atom to the force acting on the ith atom. The relations $\boldsymbol{F}_i = \sum_j \boldsymbol{F}_{i,j}$ and $\boldsymbol{F}_{i,j} + \boldsymbol{F}_{j,i} = 0$ are fulfilled. Note that the summation over j is taken over atoms within the LR associated with the respective atom i.

4. Results

4.1. Outline of the simulations

In this section, the accuracy of physical quantities is examined for various parameter sets. The tolerance on the charge neutrality $\Delta N_{\rm ele}$ is also tested because this parameter governs the number of inner iterations in every MD step. The parameter sets adopted in the present MD simulations for the liquid carbon are summarized in table 1. The first part of the table is for subsection 4.2 and the second for subsection 4.3. All MD simulations studied here with such parameter sets are numbered as in table 1. When the DM is used, only $\Delta\varepsilon$ and $\Delta N_{\rm ele}$ are shown in table 1. In the DM implemented, the Γ-point sampling is used. The TB parameters

Table 1. Summary of the parameter sets used in the present work. $t_{\rm spl}$ specifies the interval time of the data sampling.

No	N	$R_{\rm cut}$ (nm)	$\Delta\varepsilon$ (eV)	$x_{\rm max}$	$n_{\rm pl}$	$\Delta N_{\rm ele}$ (%)	$t_{\rm spl}$ (ps)
001	64	—	0.6	—	—	0.0025	4.0
002	64	0.55	0.6	50	250	1	4.0
003	64	0.55	0.75	50	200	1	3.0
004	64	0.55	1.0	50	150	1	4.0
005	64	—	0.0	—	—	—	5.0
006	512	0.55	1.0	50	150	1	3.4
007	512	0.55	0.6	50	250	0.1	3.0
008	64	0.55	0.5	100	200	0.1	7.0
009	64	0.55	0.5	100	300	0.1	4.0
010	64	0.65	0.5	100	200	0.1	4.4
011	64	—	0.5	—	—	0.0025	6.0
012	64	0.65	0.5	100	300	0.001	—
013	64	0.65	0.5	100	200	0.001	—
014	64	0.55	0.5	100	300	0.001	—
015	64	0.55	0.5	100	200	0.001	—
016	64	0.55	0.5	100	300	0.01	—
017	64	0.55	0.5	100	200	0.01	—
018	64	—	0.5	—	—	0.001	—
019	64	0.65	1.0	50	150	0.001	—

developed by Xu *et al* [13] are used in the present work. Note that the scheme of the FOEM without introducing localization reproduces the ground-state atomic configurations of small carbon clusters C_n ($n \leqslant 10$) and fullerene C_{60}. The maximum difference in bond length between the FOEM and the DM ($\Delta\varepsilon = 0$) is as small as 0.0015 nm when $\Delta\varepsilon = 0.5$ eV.

The density and temperature of the liquid carbon that we study here are 1.8 g cm^{-3} and 6000 K. The initial configurations are prepared as follows: a distorted diamond structure at the same density was heated up to 10 000 K. After equilibration for 10 000 steps (1 ps), the system was cooled down at a rate of 1 K/step (10 K fs^{-1}). The temperature control is achieved with a velocity scaling method. The relatively small time step $\Delta t = 0.1$ fs is used in subsection 4.2 and $\Delta t = 0.3$ fs in the other simulations. For each parameter set, after more than 0.7 ps of thermalization, the data for the MD simulations with the uniform interval of about 1 fs were used to compute the radial distribution function (RDF) and the atomic mean square displacement (MSD).

4.2. Structural and dynamical properties of liquid carbon

The RDF calculated by the FOEM reproduces well the result obtained by the DM. An example of comparison between two methods is shown in figure 3 for Nos 1 and 2. Note that even such a large ΔN_{ele} does not change the RDF significantly. The effects of a finite smearing width are relatively small at about $\Delta\varepsilon = 0.6$ eV. The first peak in $g(r)$ is sharpened very slightly when $\Delta\varepsilon = 0$ (No 5). However, it turns out that a larger $\Delta\varepsilon$ leads to obvious changes in $g(r)$. Figure 4 shows such effects of a finite $\Delta\varepsilon$ on $g(r)$ for larger $\Delta\varepsilon$s. For the largest $\Delta\varepsilon$ in the figure, the first and second peaks are broadened and the first minimum is raised. As shown in table 2, the ratios of variously coordinated atoms do not show remarkable differences for

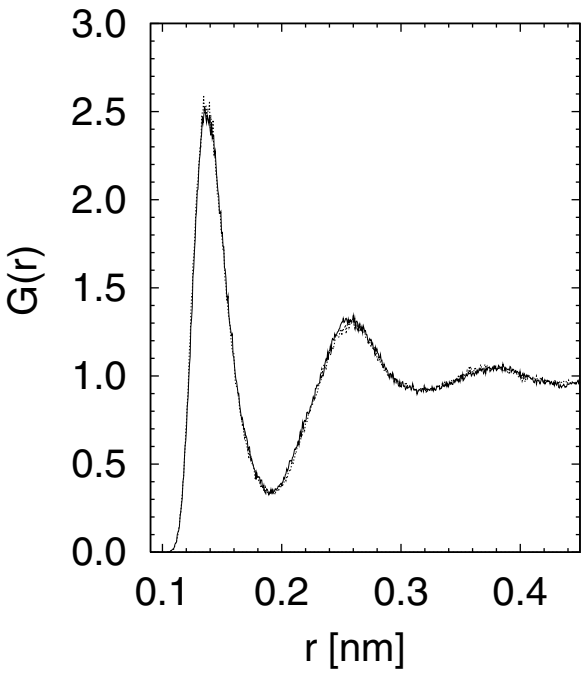

Figure 3. The radial distribution functions of liquid carbon at 1.8 g cm^{-3} and 6000 K obtained by the FOEM (full line) and the DM (dotted line) with $\Delta = 0.6$ eV.

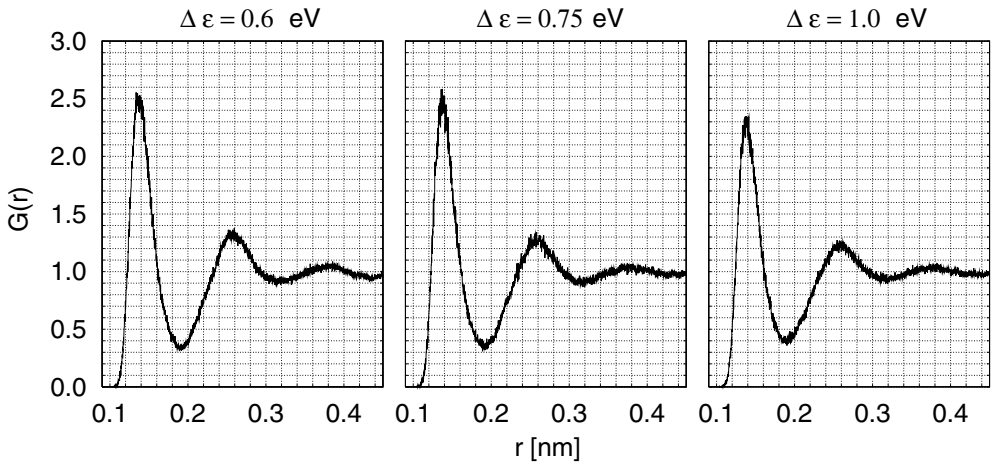

Figure 4. The dependence of the smearing width $\Delta\varepsilon$ for the RDF. From simulations No 2 (left), No 3 (centre), and No 4 (right).

Table 2. Ratios of variously coordinated atoms of liquid carbon at 1.8 g cm^{-3} and 6000 K. The values with (without) parentheses are calculated with the diagonalization method (the Fermi operator expansion). The averaged coordination number (n_c) is also shown.

Data No	$\Delta\varepsilon$ (eV)	N	Onefold (%)	Twofold (%)	Threefold (%)	Fourfold (%)	n_c
005	0.0	64	(8.4)	(53.4)	(35.6)	(2.6)	2.3
008	0.5	64	9.3	55.1	33.5	1.9	2.3
011		64	(8.5)	(53.8)	(35.5)	(2.1)	2.3
007	0.6	512	8.9	54.6	34.3	2.0	2.3
002		64	9.3	54.0	34.5	2.0	2.3
001		64	(8.4)	(54.9)	(34.4)	(2.1)	2.3
006	1.0	512	13.2	55.6	28.7	1.6	2.2
004		64	13.3	56.1	28.1	1.4	2.2

the various $\Delta\varepsilon$s used. For the largest $\Delta\varepsilon$, the number of onefold atoms increases and that of threefold atoms decreases.

$g(r)$ and the ratios of variously coordinated atoms agree with the previous result obtained by the DM for the system size of 216 atoms at the same density and temperature [12]. Also note that system size dependences of liquid carbons are not observed significantly for the quantities such as the RDF, ratios of variously coordinated atoms, averaged pressure, and MSD.

The MSD is also calculated from each MD simulation. The typical time dependence of the MSD is shown in figure 5. The linear behaviour characterizing a liquid state is observed for all cases studied here. The self-diffusion constant (SDC) of the atoms D is estimated by using the Einstein relation stating that $6D$ is equal to the slope of the linear part of the MSD. The Ds obtained are summarized in table 3 with the averaged pressures and their fluctuations. In this table, there is a tendency for a larger $\Delta\varepsilon$ to result in a larger D. For the largest $\Delta\varepsilon$, the pressure and D are increased by 65–75% from their minimum values in the table. For a physical choice of $\Delta\varepsilon$ (=0.5 eV), the data shown in table 3 are slightly scattered; this may depend on the detail of parameter sets and the fluctuation caused by the small system size.

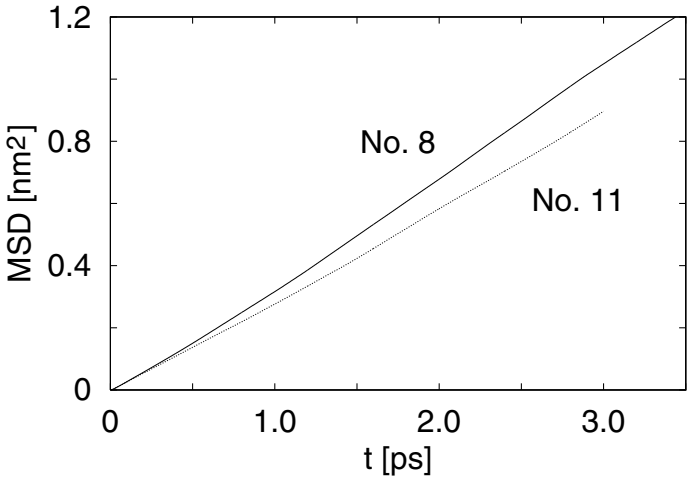

Figure 5. The mean square displacement obtained by the FOEM (full line) and the DM (dotted line) with $\Delta\varepsilon = 0.5$ eV.

Table 3. Averaged pressures P, fluctuations of pressure ΔP, and self-diffusion constants D. The values with (without) parentheses are calculated with the diagonalization method (the Fermi operator expansion).

Data No	$\Delta\varepsilon$ (eV)	N	P (GPa)	ΔP (GPa)	D (10^{-4} cm^2 s^{-1})
005	0.0	64	(3.7)	(4.7)	(4.6)
008	0.5	64	4.1	4.6	5.8
009		64	4.0	4.4	5.6
010		64	4.3	4.7	5.0
011		64	(3.7)	(4.8)	(4.6)
007	0.6	512	4.3	1.6	5.7
002		64	4.2	4.5	5.1
001		64	(4.3)	(4.5)	(4.8)
006	1.0	512	5.9	1.4	8.1
004		64	6.0	4.0	7.5

For the simulations shown in table 3, which only require a moderate computational resource, the D and the P obtained by FOEM usually give values larger by 10–20% than the values obtained by the DM. If the system size dependence is also negligible for the DM, the result of using the FOEM with a more accurate parameter set will approach the values obtained by the DM. At the end of this section, by using the most accurate parameter set, we will obtain a result very similar to that obtained by the DM.

4.3. The energy conservation

In $\mathcal{O}(N)$ approximations of the TB scheme, the conservation of energy during a constant-energy MD simulation, which is an indicator of the quality of the MD simulation, is not highly accurate. This is interpreted as showing that a good conservation of energy corresponds to a good consistency between the potential energy and the atomic forces. In order to check the

conservation of energies for various parameter sets, some MD runs were performed with a time step $\Delta t = 0.3$ fs and small tolerances $\Delta N_{\rm ele}$, because a larger $\Delta N_{\rm ele}$ gives a drastic energy drift. Changing to a smaller time step, such as $\Delta t = 0.1$ fs, does not improve the energy conservation. The time evolution of the energies with the most accurate parameter set that we studied with $\Delta\varepsilon = 0.5$ eV (No 12) is shown in figure 6. The averaged temperature of the system is about 6500 K. The conservation energy, $E_{\rm cons}$, shown at the top of figure 6 remains almost constant at least for a few picoseconds, and no fatal energy drift is observed. Both drift and fluctuation of the energy are sufficiently smaller than the fluctuations of the kinetic energy. The middle and bottom curves in figure 6 show $E_{\rm pot} - E_{\rm ent}$ and $E_{\rm pot}$, respectively. The time variation of $E_{\rm ent}$ is not remarkable, compared with that of the potential energy, which is easily seen from the time dependences of the two energies in the figure.

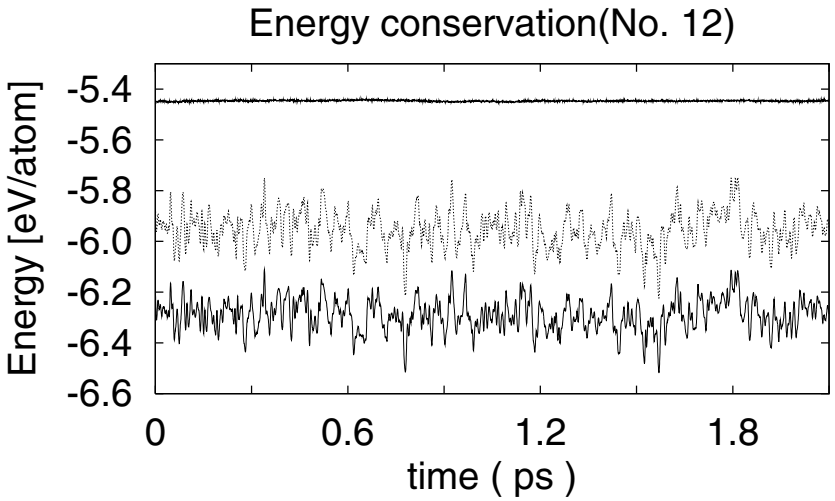

Figure 6. The time evolution of the energetics for simulation of No 12. The top, middle, and bottom curves show the conservation energy ($E_{\rm cons}$), the potential energy without the entropic energy of the electrons ($E_{\rm pot} - E_{\rm ent}$), and the potential energy ($E_{\rm pot}$).

An energy drift is obviously observed for some parameter sets, corresponding to a low-cost cpu time. When $\Delta N_{\rm ele} = 0.1$–1%, inner iterations are required for hardly any MD steps. Requiring $\Delta N_{\rm ele} = 0.001\%$, the number of inner iterations is three for all MD steps in the present implementation. Therefore, of course, the latter is more time consuming than the former. $R_{\rm cut} = 0.55$ (0.65) nm corresponds to about 62 (104) atoms in a corresponding LR. The required cpu time for one MD step for No 12 is about 7.5 times more than the cpu time for No 8. Figure 7 shows the energy conservation for various parameter sets. In this figure, large energy drifts begin to appear from 0.2 ps for No 17 and 1.1 ps for No 14. For simulations No 15 and No 16, although no large energy drift is observed, relatively large-scale oscillations begin from 1.2 and 1.1 ps, respectively. For a larger $R_{\rm cut}$, which is the case for No 11 or No 12, no large energy drift is observed. Therefore, it turns out that the MD simulation is stable for an $R_{\rm cut}$ as large as 0.65 nm.

The bottom curve in figure 7(a) is obtained from the simulation (No 19) in which the parameters are at the same level as for that of No 12 except that $\Delta\varepsilon = 1.0$ eV. The energy conservation is excellent in comparison with those for $\Delta\varepsilon = 0.5$ eV and the fluctuations are very small. This indicates that the $\mathcal{O}(N)$ approximation is substantially improved when $\Delta\varepsilon = 1.0$ eV. Such remarkable improvement is considered to originate from a rapidly damped

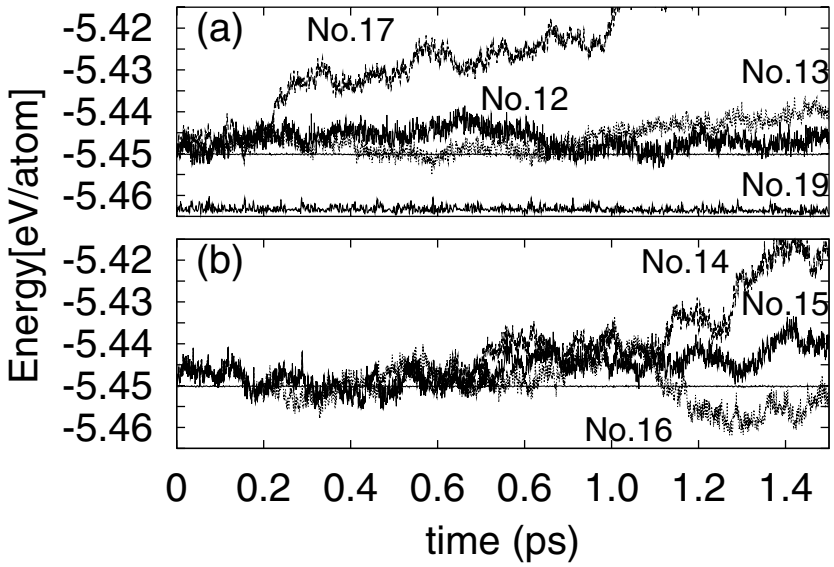

Figure 7. The energy conservation during the simulations for various parameters. Each number in the figure specifies an MD run in table 1. The straight lines around −5.45 eV/atom in (a) and (b) are obtained by the DM. The bottom line in (a), which is shifted upward by 0.5 eV/atom to show it in the figure, is obtained with $\Delta\varepsilon = 1.0$ eV (No 19).

behaviour of the projected orbital $f(x)|\varphi_{\ell\alpha}\rangle$ at a larger $\Delta\varepsilon$ because the number of polynomials is at the same level (same value of C) for both No 12 and No 19.

Before closing this section, let us point out the role of the system size in MD simulations. Even if the system size dependence on averaged physical quantities, such as the RDF, averaged pressure, and MSD, is not remarkable, it is important to note that a large system realizes a higher statistical accuracy and a smaller statistical fluctuation in thermodynamical variables. As seen in table 3, the ΔPs are even larger than the Ps for the 64-atom system. The time evolution of temporal pressures is shown in figure 8 for both 512 and 4096 atoms. The initial configuration of the latter system was constructed by replicating a system of 512 atoms and giving random velocities according to the Maxwell distribution. By comparing the values of ΔP for different system sizes, we obtained 4.6, 1.6, and 0.65 GPa for 64, 512, and 4096 atoms, respectively. On increasing the system size N, the ratio $\Delta P/P$ is suppressed in accordance with a rate of $1/\sqrt{N}$. A large system will result in more reliable thermodynamical properties of such low-density (low-pressure) systems without much ambiguity in the statistical average.

Finally, we performed a simulation with the same level of parameters as for No 12, considered as one of the most accurate parameter sets in the present work, by using the same method as in section 4.2. The values obtained for P and D are 3.6 GPa and 4.6×10^{-4} cm^2 s^{-1}, which are in good agreement with the values obtained by the DM.

5. Conclusions

The $\mathcal{O}(N)$ TB-MD is implemented with the FOEM. The various physical quantities (RDF, ratio of coordinated atoms, pressure, MSD, and SDC) are computed from the simulations for the liquid carbon (1.8 g cm^{-3}, 6000 K), which were performed with different parameter sets introduced in the $\mathcal{O}(N)$ approximation. The RDF obtained by the FOEM reproduces well

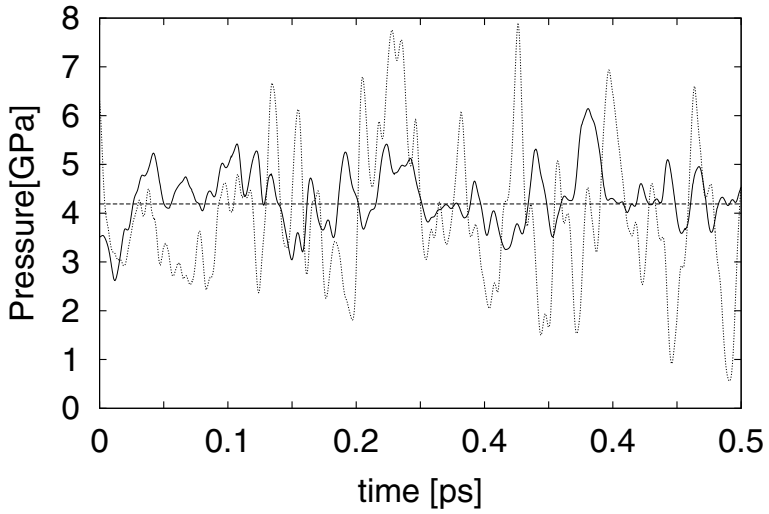

Figure 8. The time evolution of temporal pressures for both 512-atom (dotted) and 4096-atom (solid) systems.

the result obtained by the DM even when a relatively large tolerance on the charge neutrality $\Delta N_{\rm ele}$ was used. The effects of the finite $\Delta\varepsilon$ on physical quantities are observed remarkably at $\Delta\varepsilon = 1.0$ eV. In comparison with the results obtained by the DM, the pressure P and the self-diffusion constant D are obtained within 10–20% error by using a parameter set which needs only a moderate computational resource. The most accurate parameter set that we have studied here results in a good agreement with the result obtained by the DM. The energy conservation in the constant-energy simulation was examined. It was found that the energy conservation is stable for $R_{\rm cut}$ as large as 0.65 nm even when $\Delta\varepsilon = 0.5$ eV, and for a larger $\Delta\varepsilon$ a better conservation was obtained. The system size dependence is not observed for the RDF and SDC. A system as large as 4096 atoms makes fluctuations so remarkably small that it gives rise to accurate thermodynamical properties for such low-pressured liquid carbon.

Acknowledgments

The authors would like to thank Dr F Shimizu for helpful discussion about parallel computations, Dr H Shimizu for his help on the Workstation clusters, and Mrs H Miura and M Arai for their help in initial parts of this work. The calculation in this work was partially carried out using the facilities of the Supercomputer Centre, Institute for Solid State Physics, University of Tokyo. The authors also acknowledge the computational resources made available by the Centre for Promotion of Computational Science and Engineering (CCSE) of the Japan Atomic Energy Research Institute (JAERI). One of the authors (TO) would like to express thanks for financial support from a Grant-in-Aid for Scientific Research provided by the Ministry of Education, Science, Sports, and Culture, Japan. One of the authors (YH) would like to thank the JST for partial financial support.

References

[1] Li X-P, Nunes R W and Vanderbilt D 1993 *Phys. Rev.* B **47** 10 891
[2] Ordejo'n P, Drabold D A, Grumbach M P and Martine R M 1993 *Phys. Rev.* B **48** 14 646

[3] Mauri F and Galli G 1994 *Phys. Rev.* B **50** 4316
[4] Goedecker S and Colombo L 1994 *Phys. Rev. Lett.* **73** 122
[5] Goedecker S and Teter M 1995 *Phys. Rev.* B **51** 9455
[6] Stephan U and Drabold D A 1998 *Phys. Rev.* B **57** 6391
[7] Qiu S-Y, Wang C Z, Ho K M and Chan C T 1994 *J. Phys.: Condens. Matter* **6** 9153
[8] Horsfield A P, Bratkovsky A M, Pettifor D G and Aoki M 1996 *Phys. Rev.* B **53** 1656
[9] Horsfield A P, Bratkovsky A M, Fearn M, Pettifor D G and Aoki M 1996 *Phys. Rev.* B **53** 12 694
[10] Horsfield A P and Bratkovsky A M 1996 *Phys. Rev.* B **53** 15 381
[11] Bowler D R, Aoki M, Goringe C M, Horsfield A P and Pettifor D G 1997 *Modell. Simul. Mater. Sci. Eng.* **5** 199
[12] Morris J R, Wang C Z and Ho K M 1995 *Phys. Rev.* B **52** 4138
[13] Xu C H, Wang C Z, Chan C T and Ho K M 1922 *J. Phys.: Condens. Matter* **4** 6047